Dynamics of laser induced thermoelastic expansion of native and coagulated *ex-vivo* soft tissue samples and their optical and thermo-mechanical properties

Behrouz Soroushian*[a], William M. Whelan[b], Michael C. Kolios[a]
[a]Department of Physics, Ryerson University, Toronto, Canada;
[b]Department of Physics, University of PEI, Charlottetown, Canada

ABSTRACT

The interferometric measurement of laser induced thermoelastic expansion of tissue samples can be used to estimate their optical, thermal and mechanical properties. This method was used to assess the Gruneisen coefficient and optical attenuation depth for native and coagulated *ex-vivo* bovine liver and porcine kidney samples. The results demonstrate decreases of 54% and 60% in the optical attenuation depth in bovine liver and porcine kidney after coagulation, respectively. The Gruneisen coefficient of native porcine kidney was determined to be 58% smaller ($p < 0.05$) that native bovine liver. The measured Gruneisen coefficients for native and coagulated ex-vivo porcine kidney were 0.07 ± 0.03 and 0.105 ± 0.02, respectively, whereas the Gruneisen coefficients for native and coagulated liver were 0.126 ± 0.036 and 0.127 ± 0.04, respectively. Our measurements indicate significant inter sample variability due likely to inherent variations in tissue optical absorption and surface preparation.

Keywords: Thermoelastic expansion of tissue sample, surface displacement, optical attenuation depth, interferometry measurement.

1. INTRODUCTION

Optoacoustic imaging (OA) relies on the detection of transient pressure waves induced in a target after its irradiation by short laser pulses. The characteristics of the laser induced optoacoustic signal depend upon the interplay of the optical, thermal and mechanical properties of the target. Optoacoustic techniques can exploit changes in these properties when a tissue undergoes thermal treatment and therefore can be used as an effective method for assessment and help minimize damage to normal tissue [1,2]. Several previous studies have shown that changes in the optical properties of thermally treated tissues (for instance the increase in the reduced scattering coefficient) play an important role in contrast between laser induced optoacoustic signals from treated and untreated tissues [1, 3]. However the thermal treatment of tissues can also lead to changes in their thermo-mechanical properties [4]. The role of these property changes on optoacoustic contrast is less known. We recently employed an inteferometry method for studying laser induced thermoelastic deformation of tissue and tissue mimicking phantom samples. The mathematical equation governing laser induced thermoelastic expansion of a target was numerically solved. By using this technique we were able to estimate optical and thermo-mechanical properties of samples simultaneously at the same point of the sample which is very difficult to achieve with other techniques.

2. THEORY

When a short laser pulse reaches the surface of a turbid target like tissue or a tissue mimicking phantom, it enters into the medium and will be distributed inside the target because of scattering. The final distribution of light inside the target can be approximated by an axial symmetric function with an exponentially decaying axial profile and a Gaussian radial profile:

$$I(r,z) = I_0 e^{-r^2/w^2} e^{-z/D} \quad (1)$$

Photons Plus Ultrasound: Imaging and Sensing 2011, edited by Alexander A. Oraevsky, Lihong V. Wang,
Proc. of SPIE Vol. 7899, 78990Z · © 2011 SPIE · CCC code: 1605-7422/11/$18 · doi: 10.1117/12.876011

$$D = \left[3\mu_a(\mu_a + \mu_s')\right]^{-1/2} \tag{2}$$

in which μ_a and μ'_s are the optical absorption and reduced scattering coefficients of the material, respectively. The absorption of light with such a distribution profile results in generation of heat inside the target which leads to a temperature rise. One can assume that the initial temperature distribution and distribution of the absorbed light in the target are the same:

$$T(r,z) = T_0 e^{-r^2/w^2} e^{-z/D} \qquad \text{and} \qquad T_0 = \frac{\Phi\mu_a}{\rho C_V} \tag{3}$$

where C_V is the heat capacity in constant volume, Φ is the laser fluence, ρ is mass density. A nonuniform temperature distribution leads to the creation of mechanical stresses inside the target which in turn causes thermoelastic deformation of the target. The resulting thermoelastic deformation of the sample can be described by a wave equation in the form of:

$$\rho\frac{\partial^2\mathbf{u}}{\partial t^2} - \frac{E}{2(1+\sigma)}\nabla^2\mathbf{u} - \frac{E}{2(1+\sigma)(1-2\sigma)}\nabla(\nabla\cdot\mathbf{u}) = \frac{-E\beta}{3(1-2\sigma)}\nabla T(r,z) \tag{4}$$

where **u** is the displacement vector, E is Young's modulus, σ is Poisson's ratio and β is the thermal expansion coefficient of the material. Numerical solutions to equation (4) are explored using the finite-difference time domain (FDTD) method using an appropriate set of boundary conditions. The details of the method are previously described elsewhere [8]. Briefly a staggered mesh was used to discretize the space in cylindrical coordinates. The temperature distribution inside the target was assumed to be axial symmetric to simplify the calculations. An absorbing boundary layer at the distal edge of the solution geometry with rigid constraints (displacement zero at this boundary) was used to reduce artificial wave reflections from the boundary. Since the numerical solutions of the wave equation require excessive computation time and resources, they are not used to describe all of dynamics for the thermoelastic expansion. However a solution to the thermoelastic wave equation when a range of properties for biological tissues are applied leads to three distinguishable time regimes [5]; the first regime is shortly after the pulse when the internal stresses resulting from the nonuniform temperature distribution cause thermoelastic deformation of the absorbing area. The time scale of this regime is determined by the optical attenuation depth and speed of sound in the sample (for soft tissues like liver around few hundred nanoseconds). The target surface displacement during this period can be approximated by [6]:

$$u(t) = u_0\left[1 - e^{\left(-c_L t/D\right)}\right] \tag{5}$$

where u_0 which is the maximum displacement of the target surface which is determined by thermo-mechanical properties of the sample and c_L is longitudinal speed of sound in the target. After reaching its maximum displacement, the target surface sustains a quasi-steady state (the second regime). During this period, the system reaches equilibrium and although the individual stress components inside the target are not zero and even can be appreciable, the net force in any direction will be zero. For an initial temperature distribution in the form of (3) an analytical expression for the equilibrium surface displacement on the axis z during the quasi-steady-state time regime is given by [7]:

$$u_z = \frac{2(1+\sigma)}{3}\frac{\Gamma}{\rho c_L^2} g_0(R)\Phi \tag{6}$$

where $g_0(R)$ is a function dependent upon the aspect ratio R, which is given by the ratio of the laser beam radius, w, to the optical attenuation depth, D ($R = w/D$). The parameter $\Gamma = c_L^2\beta/C_V$ is the Grüneisen coefficient, an important thermo-mechanical property of the sample, which in addition to its dependence on the thermal expansion coefficient and the specific heat capacity is also dependent on the longitudinal speed of sound in the target, c_L. The Grüneisen coefficient can be determined using equation (6) by performing measurements for the equilibrium displacement of the sample surface after its exposure to laser pulses with different energies.

2.1 Measuring setup

The interferometric setup used for our experiments has been described previously [8]. Laser pulses at a 750 nm wavelength and 6.5 ns pulse duration are emitted from an optical parametric oscillator (OPO – Vibrant B-532, Opotek Inc., Carlsbad, CA, USA). These pulses with a repetition rate of 10 Hz are directed onto the target surface. By measuring the beam profile on a photographic page, the final beam size on the target location has been determined to be an elliptical cross section with major and minor axes of 5 and 3 mm respectively. A part of the pump beam was directed onto a fast silicon photodiode (DET10A, 200-1100 nm, Thorlabs, Newton, USA) to measure the pulse energy. The thermoelastic movements of the samples surface were measured using a modified Michelson interferometer. It is built around a cw solid-state laser (GCL-025-S, CrystaLaser, Reno, USA) operating at the wavelength of 532 nm. The beam from the laser was split in two parts with one directed towards a corner cube mounted on a rotating table permitting a constant modulation on the interference pattern when the target surface is not moving. The interference signals were detected by a photomultiplier (Hamamatsu H7732P-11, Hamamatsu City, Japan) and after amplification (Miteq AU-1291, Miteq, Hauppauge, USA) were digitized on an oscilloscope (Agilent DSO6054A, Agilent, Santa Clara, USA) and recorded to be analyzed later. The interference pattern was recorded during a period of 10 μs from 2 μs prior to the laser pulse incident onto the target. The resulting data were exported to Matlab for analysis. Displacement of the targets was calculated using Hilbert transform on the interferogram.

2.2 Sample preparation

Seven bovine liver samples and six porcine kidney samples (each on a different day) were purchased from a local market. The samples remained sealed in their packaging and kept at 4 °C to avoid gassing and to slow tissue degradation. From each piece of liver, two samples of about 5 x 5 x 1 cm were prepared. One of the samples was placed in a 70 °C water bath for 30 minutes. The heated samples were then removed and cut in smaller rectangular pieces with dimensions of approximately 2 x 1 x 2 cm. The untreated liver sample was also cut in smaller pieces with similar dimensions as of the heated one. The accuracy of our interferometry technique is improved for tissue samples with a smooth, flat surface. As these two surface qualities can be affected by the heating process, smaller pieces were cut from the heated samples, yielding better surface uniformity. One piece from each sample was placed in the center of two identical aluminum cylindrical containers. Larger pieces of tissue were thermally treated since the process can cause the loss of flatness and smoothness of the surfaces which are used for interferometry measurements. Since these two qualities are important for the outcome of the experiments, the quality of sample surfaces was ensured by cutting smaller pieces out of the treated larger pieces of the tissue. Gelatin (Type A, SIGMA Life Science) was dissolved in hot water and after cooling to a lower temperature around 40 °C was poured around the samples in the containers. The containers then were placed in a refrigerator at temperature of 6 °C for letting the gelatin to harden and fix the samples in place. After solidification of the gelatin, the front face of the tissue sample, which was exposed to air, was used for the interferometric experimental measurements. The same procedure was used to prepare the kidney samples. The only difference is that care was taken to ensure that pieces of kidney are cut from the cortex to minimize local inhomogeneities. In addition, the kidney samples were thermally treated for a longer time, 3 hours.

3. RESULTS AND DISSCUSSIONS

Coagulated *ex-vivo* bovine liver has an average smaller optical attenuation depth (880 ± 217 μm) compared to the native liver (474 ± 110 μm). From the interferometric measurements we found that coagulated ex-vivo porcine kidney samples similarly have an average smaller optical attenuation depth (662 ± 101 μm) compared to native kidney samples (1095 ± 201 μm). The difference between the two groups is significant ($t = 3.55$, $p < 0.01$). The difference between the optical attenuation depth for native *ex-vivo* bovine liver and porcine kidney is not significant ($t = -1.85$, $p = 0.092$).

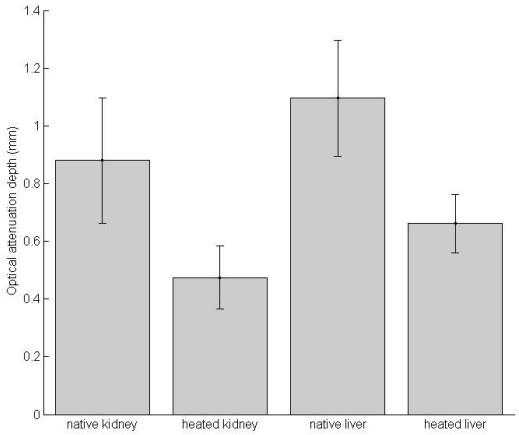

Fig 1. Average optical attenuation depth for native and coagulated *ex-vivo* bovine liver (N=7), and native and coagulated *ex-vivo* porcine kidney (N=6). Error bars are ±1 standard deviation.

We earlier reported that the interferometric measurements were unable to indicate a significant difference between values of Grüneisen coefficient for the native and coagulated liver tissues [8]. The calculated Gruneisen coefficients for native and coagulated kidney and liver are shown as a box-and-whisker diagram in the Fig. 2. The average value of the Gruneisen coefficient for both groups of the native and coagulated liver tissue samples was estimated 0.12. The difference between Gruneisen coefficient for native and coagulated porcine kidney samples is more pronounced. The measurements yield an average value of 0.07 ± 0.03 for the Gruneisen coefficient in the case of native ex-vivo porcine kidney while this value for the coagulated samples is 0.105 ± 0.02. The difference between these two groups is significant only to the level of $p = 0.091$ ($t = -1.87$). However when comparing the native kidney samples with native liver tissues, one finds that the difference between the Gruneisen coefficients for this two groups is significant ($t = -2.61$, $p < 0.05$). The Gruneisen coefficient of native kidney tissue samples is significantly smaller that native liver samples.

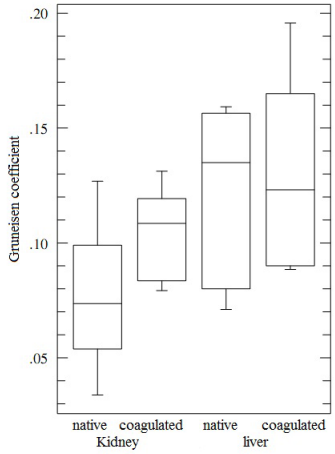

Fig 2. Calculated Gruneisen coefficients for native and coagulated *ex-vivo* bovine liver (N=7), and native and coagulated *ex-vivo* porcine kidney (N=6).

The stresses induced in the target by the light absorption and temperature rise cause the tissue surface to expand and reach a maximum displacement. However after reaching this maximum displacement the target surface may contract to a new equilibrium position. In our experiments with tissue mimicking phantoms, *ex-vivo* bovine liver and porcine kidney tissues, we observed that the coagulated samples generally have shown more prominent contractions compared to untreated samples. We earlier related this retraction behavior to differences of the mechanical properties between native

and coagulated liver tissue samples. Further work is undertaken to quantify and analyze the similar behavior in the case of native and coagulated *ex-vivo* porcine kidney tissue samples.

4. CONCLUSION

Interferometric measurements of the laser induced thermoelastic expansion of soft tissues can provide valuable information about their optical, thermal and mechanical properties. With this technique, the determination of the optical attenuation depth and Grüneisen coefficient of the tissue samples using the same tissue displacement dataset, ensures that the optical and thermomechanical properties are measured at the same tissue location. We found that the optical attenuation depth decreases significantly for coagulated porcine kidney and bovine liver compared to native tissues. In addition, the Gruneisen coefficient for coagulated porcine kidney was 33% higher than native kidney. However, no significant difference in the Gruneisen coefficient was observed for native and coagulated bovine liver. The considerable variability observed in our experiments are likely due to intrinsic differences between properties of tissues from different animals, intra sample heterogeneities and qualities of prepared sample surfaces.

Thanks are due to Arthur Worthington for his assistance in the experiments. Financial support was provided by the Atlantic Innovation Fund, the Natural Sciences and Engineering Research Council of Canada, the Canadian Institutes of Health Research (grant CHRPJ323745-60) and the Canada Foundation for Innovation (CFI). This research was undertaken, in part, thanks to funding from the Canada Research Chairs Program awarded to Michael Kolios and Whilliam Whelan.

REFERENCES

[1] Larin, K.V., Larina, I.V., Esenaliev, R.O. "Monitoring of tissue coagulation during thermotherapy using optoacoustic technique", Journal of Physics D: Applied Physics, 38 (15), 2645-2653, (2005).

[2] Arsenault M. G., Kolios M. C. and Whelan W. M., “Optoacoustic detection of thermal lesions”, Proc. of SPIE Vol. 7177, 71771V, (2009).

[3] Iizuka, M.N., Sherar, M.D. and Vitkin, I.A. "Optical phantom materials for near infrared laser photocoagulation studies", Lasers in Surgery and Medicine 25, 159-169 (1999).

[4] Kiss, M.Z., Varghese, T., Hall, T.J. "Viscoelastic characterization of in vitro canine tissue", Physics in Medicine and Biology, 49 (18), 4207-4218, (2004).

[5] Albagli, D., Dark, M., Von Rosenberg, C., Perelman, L., Itzkan, I. and Feld, M. S., “Laser-induced thermoelastic deformation: A three-dimensional solution and its application to the ablation of biological tissue.” Med. Phys., 21(8), 1323-1331 (1994).

[6] Payne B. P., Venugopalan V., Mikic B. B. and Nishioka N. S., "Optoacoustic determination of optical attenuation depth using interferometric detection", J. Biomed. Optics 8(2), 264–272 (2003).

[7] Dark M. L., Perelman L. T., Itzkan I., Schaffer J. L. and Feld M. S., "Physical properties of hydrated tissue determined by surface interferometry of laser-induced thermoelastic deformation", Phys. Med. Biol., 45, 529-539 (2000).

[8] Soroushian B., Whelan, W. M. and Kolios M. C., “Study of laser-induced thermoelastic deformation of native and coagulated ex-vivo bovine liver tissues for estimating their optical and thermomechanical properties”, J. Biomed. Opt. 15, 065002 (2010).